Strengthening Shear-Damaged Reinforced Concrete Beams Using Iron-Based Shape Memory Alloys

Miguel González-Góez, Trevor D. Hrynyk, and Eugene Kim

Abstract Advanced steel reinforcement technologies are key to enabling more durable and resilient concrete infrastructure in the face of rapidly growing demands, accelerating climate change, and extreme hazards. However, solutions for improving the performance of concrete elements in shear have historically relied on passive means where the reinforcement is only engaged after diagonal or transverse concrete cracking has occurred. This paper presents a numerical investigation on the use of prestressed iron-based shape memory alloys (Fe-SMA) to strengthen shear-damaged reinforced concrete (RC) members. Firstly, a numerical model based on test data from the literature involving large-scale shear-critical RC beams is developed using the program VecTor2. A parametric analysis is then conducted to determine the effects of externally bonded prestressed Fe-SMA on the shear response by varying the Fe-SMA and steel transverse reinforcement volume, the level of prestressing and the bidirectionality of SMA. The main focus of the analysis is on ultimate capacity and crack closing. The results of this study indicate that RC beams retrofitted using Fe-SMA exhibit reduced shear cracking and increased shear capacities.

Keywords Shear-damaged reinforced concrete · Iron-based shape · Memory alloys

1 Introduction

As a result of growing traffic demands and structural degradation accelerated by climate change, there is a critical need for continued advancement of concrete repair and strengthening technologies to enable extended bridge service life. The 2019 Canadian Infrastructure Report Card indicates that over 10% of the nation's bridges are in poor or very poor condition, and that number is forecast to grow in the coming

M. González-Góez (✉) · T. D. Hrynyk · E. Kim
Department of Civil and Environmental Engineering, University of Waterloo, Waterloo, Canada
e-mail: m32gonza@uwaterloo.ca

decades. In response, several retrofit strategies involving externally bonded materials have been developed for reinforced concrete (RC) structures such as fibre-reinforced polymers (FRPs) and near-surface mounted (NSM) steel components. Although many techniques have been developed for enhancing the in-service flexural performance and durability of RC members under flexure-dominated loading scenarios (e.g., the application of prestressing to reduce concrete cracking), comparatively fewer practical options are available to mitigate transverse, or shear, crack development in RC bridge elements. In addition to that, most transverse strengthening techniques are passive in nature and are only engaged after significant damage development. Alternatively, active transverse reinforcement strategies could be used to induce compressive stresses within the surrounding concrete and, as a by-product, potentially close, or at least reduce the widths of, existing cracks and prevent further shear-related concrete damage from occurring, thus enhancing member durability, maintaining member stiffness, and potentially increasing member shear resisting capacity.

The objective of this study is to numerically examine the effectiveness of Fe-SMA as an active strengthening method in shear-damaged RC beams. An experimental specimen presented in the literature and involving a full-scale conventional RC pier cap element was modelled using the nonlinear finite element analysis (NLFEA) software program VecTor2 [16]. Prestressed Fe-SMA elements were introduced in the model to simulate the addition of transverse reinforcement strengthening, and a parametric analysis was performed to investigate the influence of various SMA reinforcement parameters that are expected to play key roles on strengthened component shear resisting performance: (i) the Fe-SMA reinforcement ratio, (ii) the level of SMA prestressing, (iii) the orientation of the simulated SMA retrofit, and (iv) the presence of conventional internal transverse reinforcement (i.e., steel stirrups). The findings of this paper provide insight, generated by way of numerical modelling, into the shear resisting performance of RC components employing novel active shear-strengthening techniques and also illustrate cost-effective modelling strategies that can be utilized to investigate other, or similar, shear retrofits.

2   Shape Memory Alloys

Shape memory alloys (SMAs) are a class of smart materials that undergo phase transformations under mechanical and thermal loading. SMAs possess two unique thermomechanical properties: (1) superelasticity, which is the ability to recover its shape after large nonlinear strains, and (2) shape memory effect, which allows prestrained (i.e., predeformed) SMAs to fully recover plastic deformations and return to their original shape by increasing their temperature. Use of the shape memory effect for prestressing and active confinement has already been demonstrated in numerous research studies using nickel-titanium (Ni–Ti) SMA, which is the most widely available commercially [4, 11]. However, the cost of Ni–Ti is arguably prohibitive for most real-world structural engineering applications; thus, to date, it has primarily
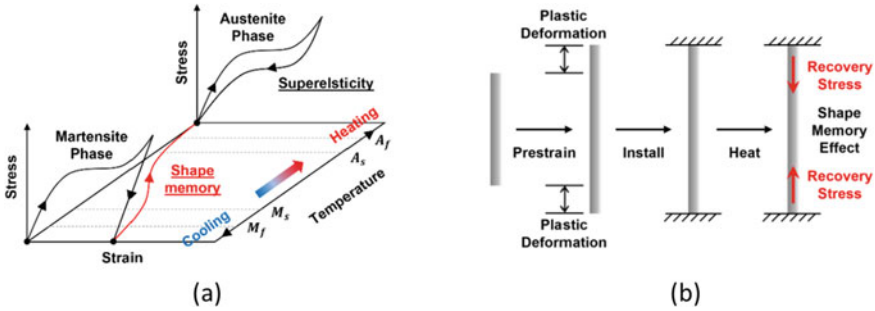
Fig. 1 **a** Thermomechanical behaviour of SMA and **b** SMA prestressing concept

been heavily utilized in other fields (e.g., medical devices, aerospace materials), but the exploration of its use for structural applications has generally been limited to specialized, and highly localized, connection regions. In contrast, iron-based SMAs (Fe-SMAs) are cheaper and easier to machine, opening the possibility of fabricating low-cost structural devices. Although Fe-SMAs do not possess superelastic properties, their shape memory effect can produce high recovery stresses (>300 MPa) at reasonable temperatures (~200ºC) which can actively confine or prestress structural members. By installing prestrained Fe-SMA strips in the transverse direction then activating the shape memory effect, an active pressure can be introduced to help close cracks and apply a confining stress in the concrete. Figure 1 illustrates the shape memory effect and the SMA prestressing concept.

Previous research has evaluated the potential of Fe-SMAs for strengthening RC structures. Soroushian et al. [12] first demonstrated the potential for Fe-SMA shear strengthening by using externally mounted Fe-SMA rods to restore the load carrying capacity of a shear-damaged RC beam. Rojob and El-Hacha [9] proposed a prestressing technique with Fe-SMAs for enhancing the flexural behaviour of RC beams and found significant increases in flexural capacity and ductility of the tested beams. In recent years, several experiments have been conducted with addition of Fe-SMA transverse reinforcement. Cladera et al. [2] presented a series of experiments on real-scale RC beams strengthened with Fe-SMA strips that showed shear strength increases on the order of 30% and delayed shear crack development as a result of the active confining stress. Czaderski et al. [3] developed a shear retrofit method using externally installed Fe-SMA stirrups and found that the transverse prestressing increased the cracking load and reduced the widths of shear cracks. The results obtained from both of these studies show that Fe-SMA prestressing is a promising retrofit strategy for mitigating concrete damage and improving the performance of shear-deficient RC components. However, the methods explored to date are not overly practical, requiring highly invasive installation procedures and anchorages, as well as lacking generally protection against environmental deterioration.

3 Preliminary Validation and Benchmark Analysis

VecTor2 [16] is a RC-dedicated NLFEA program. Cracked concrete material modelling is based on the on the formulations of the Disturbed Stress Field Model (DSFM) [14], which is an extension of the Modified Compression Field Theory (MCFT) [15]. The program is suitable for the analysis of two-dimensional RC membrane structures subjected to quasi-static or dynamic loading. A total load, secant stiffness-based, solution procedure is used and provides stable solutions for all stages of response, making VecTor2 particularly appealing for the analysis of shear-sensitive structures that tend to exhibit abrupt changes in material stiffness and response and are often governed by highly brittle failure mechanisms. Second-order effects and other concrete and reinforcement-related mechanisms that are not inherently accounted for in the formulations of the DSFM (e.g., concrete confinement and dilatation, plain concrete tension softening, concrete and steel hysteretic responses) are considered in the analysis, making the program suitable for a broad range of RC elements and analysis scenarios. In this paper, NLFEA of large-scale beam-type elements are carried-out using VecTor2. The geometry and reinforcement details of the beams are based on those from the testing program reported in Jirsa et al. [7] and [10], which entailed the testing of RC bridge pier cap girders strengthened with carbon fibre-reinforced polymer shear retrofits. In the present study, an experimental control test specimen referred to as D-U-VN-HN* was used as a benchmark for assessing relative performance of Fe-SMA shear retrofitted components and also for validating the overall suitability of the finite element meshing, material models employed, and analysis strategy.

An illustration showing the control beam geometry and reinforcement detailing is summarized in Fig. 2. The beam was constructed with a square cross section measuring 813 by 813 mm, and a total length of roughly 8.4 m. The beam was designed such that the test span region (see Fig. 2) would govern the capacity of the member and would be controlled by shear failure mechanisms. Two-legged 16-mm diameter stirrups were placed at a spacing of 457 mm, resulting in a shear reinforcement ratio of 0.11% within the test span, which is on the order of recommended minimum shear reinforcement requirements in modern North American provisions [1]. 11 US No. 11 bars were provided as longitudinal flexural reinforcement on both the tension and compression sides of the cross section resulting in a flexural tension and compression reinforcement ratio of 1.9%. The beam was tested using a skew-symmetric loading configuration that produced an inflection point at the midspan of the test span region, thus resulting in a double-curvature bending scenario. Additional details regarding the beam geometry and reinforcement, and the testing procedure used in the experimental program, are available in Jirsa et al. [7].
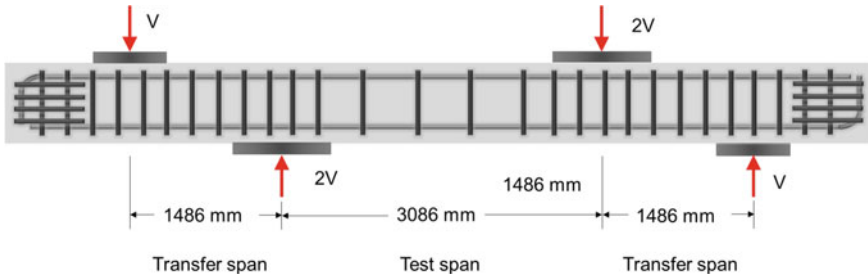
Fig. 2 Jirsa et al. [7] double-curvature control beam

3.1 Modelling Approach

Figure 3 presents the two-dimensional finite element mesh developed for the Jirsa et al. [7] RC control beam. In total, the finite element mesh consisted of 1,266 rectangular finite elements that were used to represent different reinforced concrete material types, steel bearing plates, and load/support interface regions. Flexural longitudinal reinforcement was modelled explicitly using 408 truss bar finite elements that were assumed to be perfectly bonded with the surrounding concrete. All transverse reinforcement was modelled in a smeared sense, using different RC material types to represent the different transverse reinforcement ratios provided over the length of the beam. The analysis was performed in a displacement-controlled manner, with equal and opposite displacements applied at the interior load bearing locations, and a roller and pin support reaction were provided at the two exterior bearing locations. Note that self-weight of the RC beam was neglected.

All user-definable material models and analysis parameters corresponded with VecTor2's default modelling options. More specifically, no effort was made to parametrically define models or refine analysis results, and user input was limited to the definition of the concrete and steel reinforcement materials properties, which were specified to match those reported in Jirsa et al. [7]. For reference, the concrete material
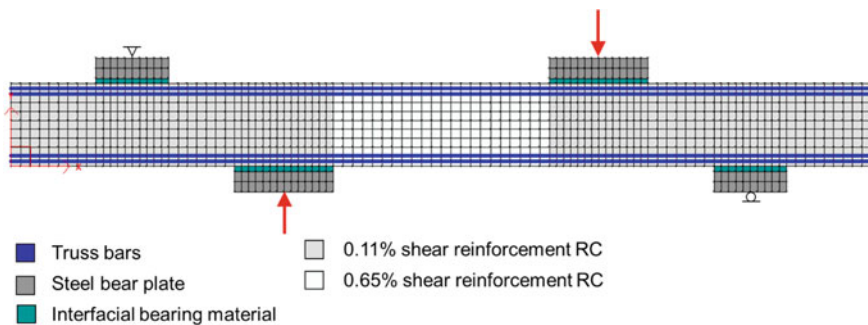

Fig. 3 VecTor2 two-dimensional model

was defined with a cylinder strength of 31 MPa and a maximum nominal aggregate size of 25 mm. Flexural reinforcement was assigned a yield strength of 420 MPa and a modulus of elasticity of 200,000 MPa. Shear reinforcement was assigned a yield strength of 400 MPa and a modulus of elasticity of 200,000 MPa.

3.2 Validation for Benchmark RC Beam

To validate the effectiveness of the meshing and behavioural models employed, results in the form of applied shear versus loading point displacement are presented in Fig. 4 and compared to the reported experimental data. From the figure, it can be seen that the shear capacity is estimated within 5% of that reported. Further, it can be seen that the finite element model developed was generally capable of capturing all aspects of the reported response ranging from the post-cracking shear stiffness, the capacity of the RC beam, and the brittle shear-governed failure mode encountered.

4 Parametric Study

In this section, a parametric study is performed to investigate the impacts of introducing externally bonded Fe-SMA retrofit to shear-damaged RC beams. The base geometry is the based on the pier cap test beam described in Sect. 3. Parameters selected to investigation include the amount of transverse Fe-SMA reinforcement in the test span, the level of Fe-SMA prestressing, the presence of existing internal transverse reinforcement, and addition of longitudinally oriented Fe-SMA within the web region of the beam and in the amount of 0.10%. Table 1 summarizes the parameters considered in the study.
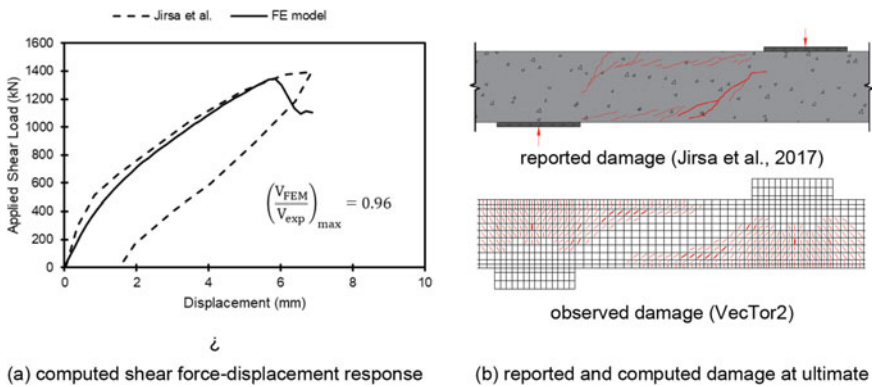

(a) computed shear force-displacement response

(b) reported and computed damage at ultimate

Fig. 4 Results for Shekarchi et al. RC control beam

Table 1 Summary of parameters considered

Prestress level (MPa)	Fe-SMA reinf ratio (%)	Fe-SMA direction	Existing shear reinf ratio
266	0.10	Vertical only	No. Reinf
399	0.20	Vertical + Horizontal	Min = 0.083%[a]
	0.30		
	0.40		

[a]Computed according to clause 11.2.8.1, CSA A23.3:19

To simulate the presence of initial shear damage that would prompt the need for shear retrofitting, and to subsequently estimate the effectiveness of the different Fe-SMA retrofits, the NLFEA was performed in three phases: (1) *initial loading*: a seed model of the RC beam was first loaded up to approximately 85% of the peak capacity to induce shear damage/distress in the RC component (see Fig. 5a), (2) *unloading*: the beam was then unloaded to 50% of the initially applied load (see Fig. 5b), (3) *retrofit and reloading*: at this point, prestressed Fe-SMA reinforcement was added within the previously defined test span region (see Fig. 2) as smeared reinforcement and the analysis was resumed until failure was estimated to occur (see Fig. 5c). Figure 5 presents a schematic view of the three-phase progression of analyses performed.

The Fe-SMA was added to the model as smeared reinforcement in the test span of the beam (see highlighted region in Fig. 6). Shape Memory Alloy (type 2) material from the VecTor2 library was used to define the constitutive models governing the response of the Fe-SMA retrofit and its associated material properties were defined to match those reported by [6] (yielding stress = 463 MPa, ultimate tensile strength = 863 MPa, and modulus of elasticity = 133,000 MPa). The Fe-SMA behaviour is shown in Fig. 7.
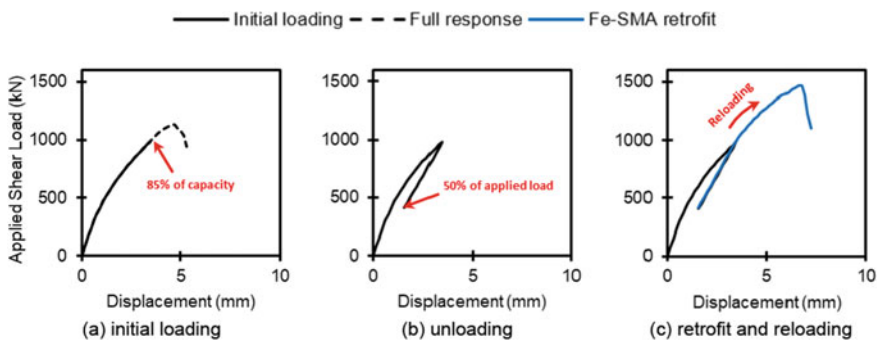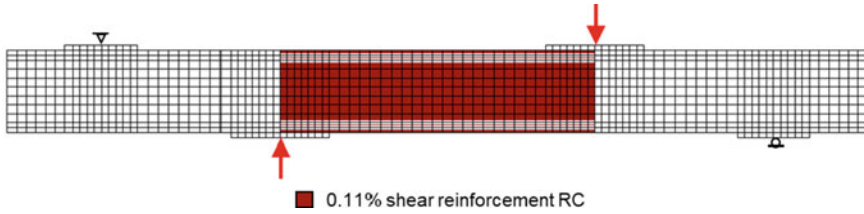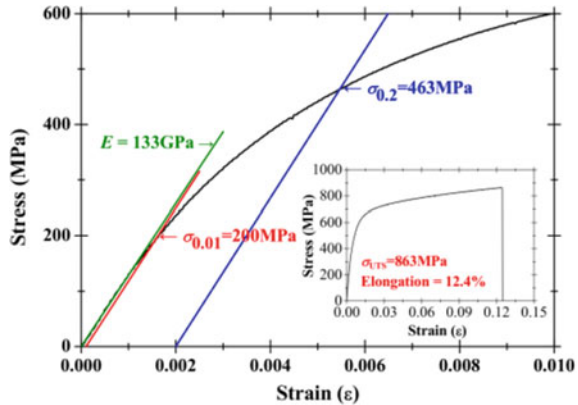

Fig. 5 NLFEA loading phases

Fig. 6 VecTor2 mesh with smeared Fe-SMA retrofit

Fig. 7 Fe-SMA stress–strain response [6]

5   Results and Discussion

The analyses were performed using four different finite element seed models to represent the varying levels of internal transverse reinforcement and the different directions/orientations of external Fe-SMA reinforcement. The seed models were denoted as VN, VT, BDN, and BDT where V = vertical Fe-SMA, BD = bidirectional Fe-SMA, N = No transverse reinforcement, and T = minimum transverse reinforcement.

5.1   Shear Response

Figure 8 presents the applied shear versus displacement results before and after Fe-SMA retrofits were incorporated into the models. It can be observed that as the external shear reinforcement ratio (ρ_v) is increased, shear capacity and displacement at peak shear resistance increased. A slight increase is also obtained by way of the transverse prestressing applied via the Fe-SMA; however, when contrasted with the impact of shear reinforcement ratio, increase the level of Fe-SMA prestressing from 286 to 399 MPa is estimated to be less significant to shear capacity. The

post-retrofit stiffness was found to follow the unloading curve of the seed models and exhibited only marginal softening after reaching and exceeding previous load levels. Results pertaining to shear capacity and corresponding shear strength gains compared to seed model analyses without any form of shear retrofit are summarized in Table 2. Maximum estimated shear strengths were 1135 kN for the models without internal transverse reinforcement (VN, BDN) and 1293 kN for models with transverse reinforcement (VT, BDT).

Additional models were developed to further investigate the impact of different shear reinforcement prestressing levels on the shear response of the beam. Figure 9 presents computed shear force–displacement responses for the VN seed model with a Fe-SMA shear retrofit of 0.10%, and Table 3 summarizes the shear capacities obtained for the different retrofits. Five different Fe-SMA prestressing levels were considered: 0, 133, 266, 333, and 399 MPa. From the data presented, it can be seen that the prestressing level does indeed enhance the shear resisting performance of the beam by way of delaying stiffness degradation and by increasing shear capacity.
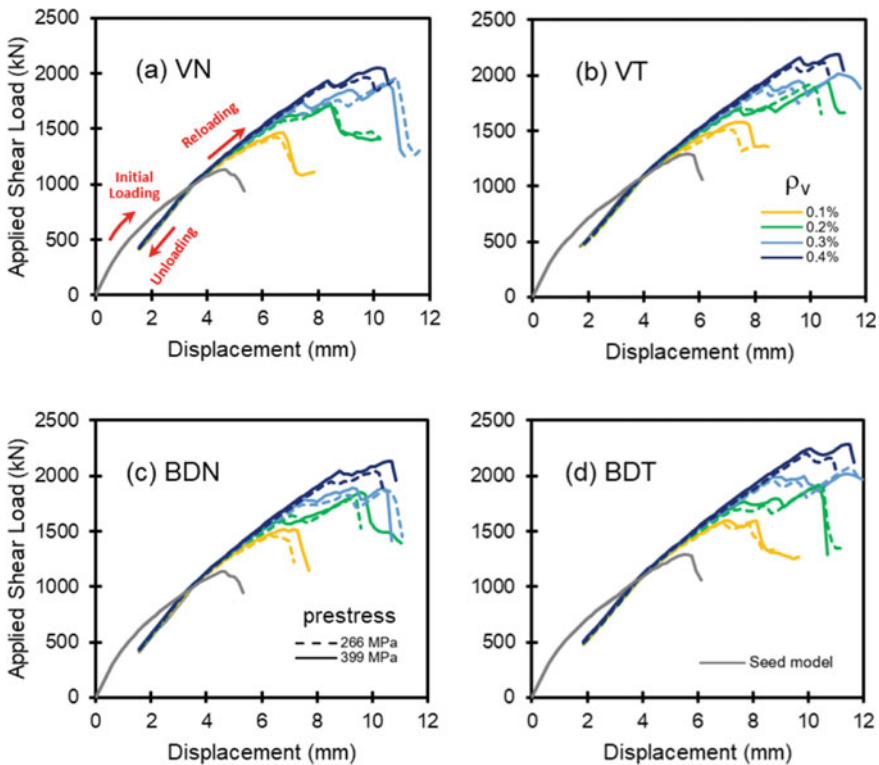

Fig. 8 Shear response

Table 2 Peak shear capacities and retrofit strength gains

| Seed model	Prestressing level (MPa)	Fe-SMA reinforcement ratio							
		0.1%	0.2%	0.3%	0.4%	0.1%	0.2%	0.3%	0.4%
		Peak shear (kN)				Peak shear increase (%)			
VN	266	1429	1736	1962	2102	26	53	73	85
	399	1466	1716	1908	2013	29	51	68	77
VT	266	1509	1924	2012	2169	17	49	56	68
	399	1581	1943	2012	2190	22	50	56	69
BDN	266	1459	1800	1873	2078	29	59	65	83
	399	1516	1849	1893	2134	34	63	67	88
BDT	266	1583	1910	2070	2204	22	48	60	70
	399	1601	1919	2018	2285	24	48	56	77
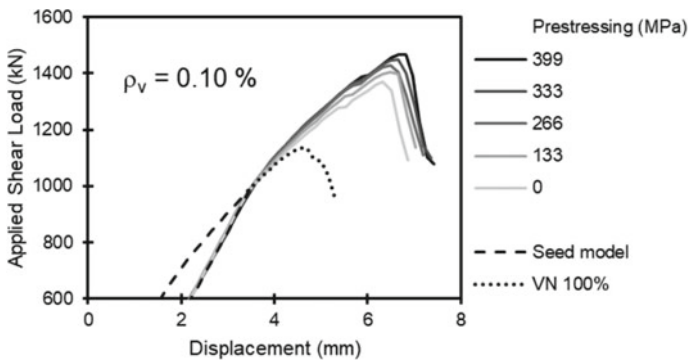
Fig. 9 Influence of prestressing level (VN seed model)

Table 3 Peak shear capacity and influence of prestressing level

Prestressing (MPa)	0	66.5	133	199	266	333	399	465	532
Equivalent prestrain ($\times 10^{-3}$)	0	0.5	1.0	1.5	2.0	2.5	3.0	3.5	4.0
Shear capacity (kN)	1370	1386	1406	1420	1429	1450	1466	1475	1475
Shear strength increase (%)	21	22	24	25	26	28	29	30	30

5.2 Crack Closing Potential

Figure 10 shows the computed crack closing response of a single finite element that is estimated to occur as a result of clamping action developed by way of the active prestressing. The selected element was located at one of the shear cracks of the seed model before retrofit, as shown in Fig. 11. The effectiveness of the Fe-SMA retrofits in closing shear cracks is clearly evident in even the lowest volume of external
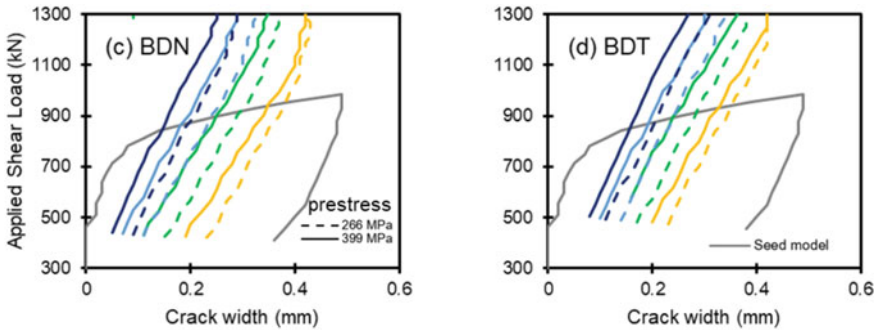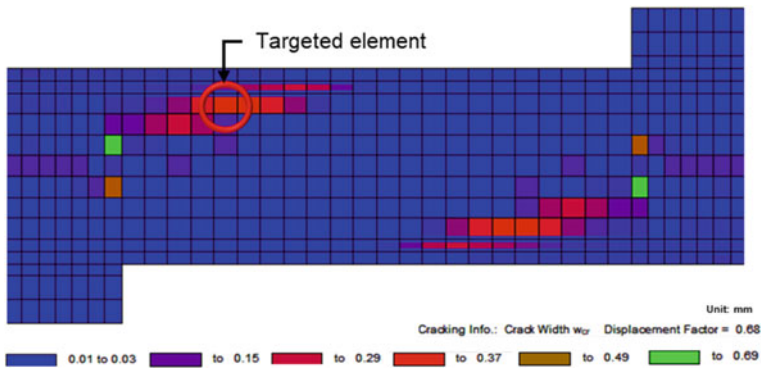
Fig. 10 Crack width in a single element

Fig. 11 Crack widths in test span before prestressed Fe-SMA addition

reinforcement. As the reinforcement ratio increases, shear crack widths are reduced by up to 88%.

The influence of prestressing level on the cracking reduction is clearly apparent in Fig. 11, with estimated shear crack widths being significantly smaller for retrofits employing higher prestressing levels (e.g., 399 MPa). Moreover, a major benefit of introducing transverse prestressing in the RC beams is the potential that cracking may be better-controlled and mitigated such they are closed and remain small, under routine service load levels. Overall, the findings of these numerical results indicate that the presence of externally bonded Fe-SMA retrofits is able to provide significant improvements in the shear resisting performance of large-scale RC beams. However, further experimental research is required to establish the viability of the proposed method and to explore different bonding techniques to incorporate Fe-SMA into the surface of the concrete.

6 Conclusions

A numerical study was conducted to evaluate the influence of several parameters on the shear resisting performance of RC beams. The results of this investigation showed that the presence of prestressed iron-based shape memory alloys on the surface of the beams can provide several improvements, which are summarized as follows:

- Iron-based shape memory alloy (Fe-SMA) retrofits were estimated to provide stiffness and strength improvements in damaged RC components as a result of the transverse prestressing induced by way of the active retrofit strategy.
- In the same manner as expected with similar retrofit methods involving passive techniques, the shear capacity of damaged shear-critical beams was estimated to increase as more transverse reinforcement was provided. Combinations of large shear reinforcement ratios with high levels of transverse prestressing provided the largest shear strength gains.
- The additional of prestressed Fe-SMA retrofits were estimated to reduce (i.e., close) shear crack widths and mitigate the development of subsequent shear crack width growth.

References

1. American Association of State Highway and Transportation Officials (2019) AASHTO LFRD bridge design specifications
2. Cladera A, Montoya-Coronado LA, Ruiz-Pinilla JG, Ribas C (2020) Shear strengthening of slender reinforced concrete T-shaped beams using iron-based shape memory alloy strips. Eng Struct 221. https://doi.org/10.1016/j.engstruct.2020.111018
3. Czaderski C, Shahverdi M, Michels J (2021) Iron based shape memory alloys as shear reinforcement for bridge girders. Construct Build Mater 274. https://doi.org/10.1016/j.conbuildmat.2020.121793
4. El-Tawil S, Ortega-Rosales J (2004) Prestressing concrete using shape memory alloy tendons. ACI Struct J 101(6):846–851
5. Federation of Canadian Municipalities (2019) The 2019 Canada Infrastructure report card
6. Hong K, Lee S, Han S, Yeon Y (2018) Evaluation of Fe-based shape memory alloy (Fe-SMA) as strengthening material for reinforced concrete structures. Appl Sci (Switzerland) 8(5). https://doi.org/10.3390/app8050730
7. Jirsa JO, Ghannoum WM, Kim CH, Sun W, Shekarchi WA, Alotaibi NK, Pudleiner DK, Zhu J, Liu S, Wang H (2017) Use of carbon fiber reinforced polymer (CFRP) with CFRP anchors for shear-strengthening and design recommendations/quality control procedures for CFRP anchors. https://library.ctr.utexas.edu/ctr-publications/0-6783-1.pdf
8. Montoya-Coronado LA, Ruiz-Pinilla JG, Ribas C, Cladera A (2019) Experimental study on shear strengthening of shear critical RC beams using iron-based shape memory alloy strips. Eng Struct 20. https://doi.org/10.1016/j.engstruct.2019.109680
9. Rojob H, El-Hacha R (2017) Self-prestressing using iron-based shape memory alloy for flexural strengthening of reinforced concrete beams. ACI Mater J 114(2):523–532. https://doi.org/10.14359/51689455
10. Shekarchi WA (2016) Shear behavior of reinforced concrete bridge pile cap girders strengthened with carbon fiber reinforced polymer (CFRP) strips and CFRP anchors

11.	Shin M, Andrawes B (2010) Experimental investigation of actively confined concrete using shape memory alloys. Eng Struct 32(3):656–664. https://doi.org/10.1016/j.engstruct.2009.11.012
12.	Soroushian P, Ostowari K, Nossoni A, Chowdhury H (2001) Repair and strengthening of concrete structures through application of corrective posttensioning forces with shape memory alloys 1770:20–26. https://doi.org/10.3141/1770-03
13.	Standards Council of Canada (2019) CSA A23.3:19, Design of concrete structures
14.	Vecchio FJ (2000) Disturbed stress field model for reinforced concrete: formulation. J Struct Eng 126(9):1070–1077. https://doi.org/10.1061/(ASCE)0733-9445(2000)126:9(1070)
15.	Vecchio FJ, Collins MP (1996) The modified compression-field theory for reinforced concrete elements subjected to shear. ACI J 83(22):219–231
16.	Wong PS, Vecchio FJ, Trommels H (2013) VecTor2 and Formworks user's manual 2nd edition